Electronic Supplementary Information

Structure determined charge transport in single DNA molecule break junctions

Kun Wang,[a] Joseph Hamill, [a] Bin Wang,[a] Cunlan Guo,[a] Sibo Jiang,[b] Zhen Huang [b] and Bingqian Xu* [a]

[a] Single Molecule Study laboratory, College of Engineering and Nanoscale Science and Engineering Center, University of Georgia, Athens, GA 30602, USA.

[b] Department of Chemistry, Georgia State University, Atlanta, GA 30303, USA

*To whom correspondence should be addressed: *email:* bxu@engr.uga.edu

S1. Experimental Details

Chemicals and materials

Oligonucleotides treated with HPLC purification (purity>85%) were ordered from Integrated DNA Technology (IDT, Coralville, IA, USA). The single strand DNA sequences of two DNA duplexes used for conductance measurements are 5'-CGCGCGCG-3' and 5'-CGCGAAACGCG-3', both with thiol group modified at 3' end respectively. Short strand (8 and 11 base pairs) of DNA molecules (5'-CGCGCGCG-3'and 5'-CGCGAAACGCG-3') was chosen because it has less possibility in structural bending and rolling. More importantly, SPMBJ technique prefers highly conducting molecules. The increase in molecule length will exponentially decrease the conductivity of the molecule, which denies the choice of long DNA molecules. Sequence of poly $d(GC)_n$ was chosen for the fact that it can be easily transformed from one to another conformation under appropriate buffer condition, which makes it a commonly used sequence for DNA secondary structure variation study. Single

strand DNA was stored in PBS (10mM phosphate, 100mM NaCl, pH 7.4) at -20˚C before use.

$MgCl_2$ was chosen to control counterion concentrations in buffer solutions. Although some other counterions like Na^+ and K^+ have been reported to successfully access DNA conformational variation, their relatively weak ionic strength,[1, 2] requesting a very high ionic concentration (>5M) to complete the variation for a short DNA duplex like ours, makes them inappropriate for precise electrical measurements at single-molecule level. Due to the high ionic strength of Mg^{2+} counterions, narrower concentration window is necessary to complete a full conformational transition, qualifying $MgCl_2$ a proper choice for our experiments. A series of different amounts of $MgCl_2$ was dissolved into PBS to produce buffer solutions with different $MgCl_2$ concentrations. Final sample solution at a specific concentration was obtained by adding single strand DNA to buffer solution with this concentration of $MgCl_2$. Then the sample solution was heated up to 90˚C in a water bath. Kept in dark, the solution temperature naturally dropped back to room temperature within 2hs and the complementary duplex was formed. The concentration of DNA duplex is 3μM for all conductance measurements. The melting temperature for both DNA sequences in solutions containing $MgCl_2$ concentrations within a range like ours is at least above 50˚C. And the higher the ionic concentration, the higher the melting temperature will be. As all electrical measurements were conducted under room temperature (~23˚C), it is hardly possible that the temperature of a single-molecule junction increased above this melting temperature even considering local heating effect.[3] Thus, we presume that the conductance measurements were mostly conducted for DNA duplexes.

The acquired DNA duplex sample solution was dropped on a freshly hydrogen flame annealed Au(111) surface for 40 min incubation. After the incubation, the conductance measurement was immediately performed.

STM imaging and electrical measurement setup

STM imaging and conductance measurements were conducted in DNA solutions containing different concentrations of $MgCl_2$ by a PicoPlus SPM system (Molecular Imaging) with a PicoScan 3000 Controller (Molecular Imaging). Sheared gold wire with diameter of 0.25 mm

(99.999%, Alfa Aesca) was used as a STM tip. To avoid ionic conduction, the STM tip was coated with Apiezon wax to keep ionic leakage current below 1pA. The obtained STM images were processed by WSxM software.[4]

The conductance measurement was carried out under 0.3V at room temperature (~23˚C) by SPM break junction technique (SPMBJ). Upon this technique, the STM tip was initially driven by piezoelectric transducer (PZT) to approach the DNA duplex monolayer on Au substrate until the current reached a preset value which implied the formation of Au-DNA-Au junctions. Then the tip retracted so that current-distance trace was recorded simultaneously. For SHM SPMBJ, a 33 ms period of pause was set for every 0.6 nm retracting distance in SHM so that steady molecular junctions were consequently generated. For both CSM and SHM, the tip kept retracting until every molecular junction was completely broken. This technique also guarantees that the single-molecule conductance was always measured at a junction conformation where a DNA molecule was approximately perpendicular to the surface right before the junction broke. It is possible that small amounts of DNA molecules might lay on the Au substrate before the junction was formed, although STM imaging suggested that most molecules were standing up on the surface. Conductance histograms were created from around 1000 individual conductance traces for each Mg^{2+} concentration. The first, most prominent peak in the histogram represents the conductance of a single DNA molecule in the break junction.

As the experiment proceeds, water evaporates from the solution, which will increase the Mg^{2+} concentration in the solution. To avoid the influence from the increase of Mg^{2+} concentration on the final results, all the data were collected within one hour so that little variation in Mg^{2+} concentration in the solution was guaranteed.

Log-Scale Conductance measurements using a log scale STM scanner was conducted in 1M $MgCl_2$ buffer solution where DNA molecules in multiple conformations could coexist. After choosing a flat area of DNA monolayer with the aid of imaging, conductance measurement was immediately performed under CSM. The retraction speed was 10nm/s. One set of data contained 122 traces and total ten sets of data were collected for histogram construction.

Linear-scale Using a linear STM scanner, conductance measurements was applied at all $MgCl_2$ concentrations under both CSM and SHM. Since we applied two specific

measurement regions: window 1 (1V/div) and 2 (50mV/div), data collecting for two windows at each concentration were performed by switching windows alternatively. It means we switched to window 2 for another set of data right after collecting one set of data under window 1, and then switched the scale back to 1V/div. By consecutively operating this way, the influence of concentration variation with measurement time going was minimized and data collected from two windows was under a relatively same condition. The tip retracting speed was 18nm/s. The retracting speed difference between the log and linear scanner was due to nothing but optimizing conductance measurement parameters. One set of data contained 122 traces and total ten sets of data were collected for histogram construction under either window. After analysis, each plateau contributed similar counts (~2000) to the histogram.

Circular dichroism (CD) measurement Setup

CD measurement was performed by JASCO J-810. DNA concentration 5μM was used for significant CD signal. The preparation procedure of DNA samples was the same as conductance measurement except for DNA concentration difference. Each single CD spectra was plotted by averaging the results of three consecutive measurements in the corresponding sample solution.

S2. DNA structure simulation

In **Fig. 6** of the main text, Z-form DNA conformation was constructed with the help of w3DNA web server.[5] The 5' and 3' terminals of the w3DNA sequence were modified in order to agree with the CGCGCGCG sequence used in this paper. This modification and all later molecular graphics images were produced using the UCSF Chimera package from the Computer Graphics Laboratory, University of California, San Francisco (supported by NIH P41 RR-01081)[6]. The B-from conformation with the same sequence was constructed with Amber 11[7]. Both B-form and Z-form DNA conformations have been neutralized and put into the explicit solvent box TIP3P and equilibrated with the experimental conditions (300 K and 1 atm pressure) for 2 ns.

S3. Two-dimensional correlation histogram

Two-dimensional correlation histograms (2DCH) outlined by Makk et al[8] were plotted in **Fig. 3a and 3b**. A 2DCH performs a calculation on each legitimate trace of a data set to compare the correlation of each data point with all the other data points in the trace. The color at the locus of two conductance values on the 2DCH is the correlation between those two conductance values as calculated by all the traces in the sample (anti-correlation in blue, correlation in red, no correlation in green). In our case, the 2DCH for each concentration reveals a broad area (circled area) of anti-correlation in the regions of multiples of the first conductance peak for both window scales as shown in **Fig. 3a and 3b** of the main text. It reveals an interesting situation that under SHM we were obtaining conductance traces with plateaus possessing only one rather than a few consecutive integer multiples of the last single Au-DNA-Au junction plateau.

S4. STM imaging

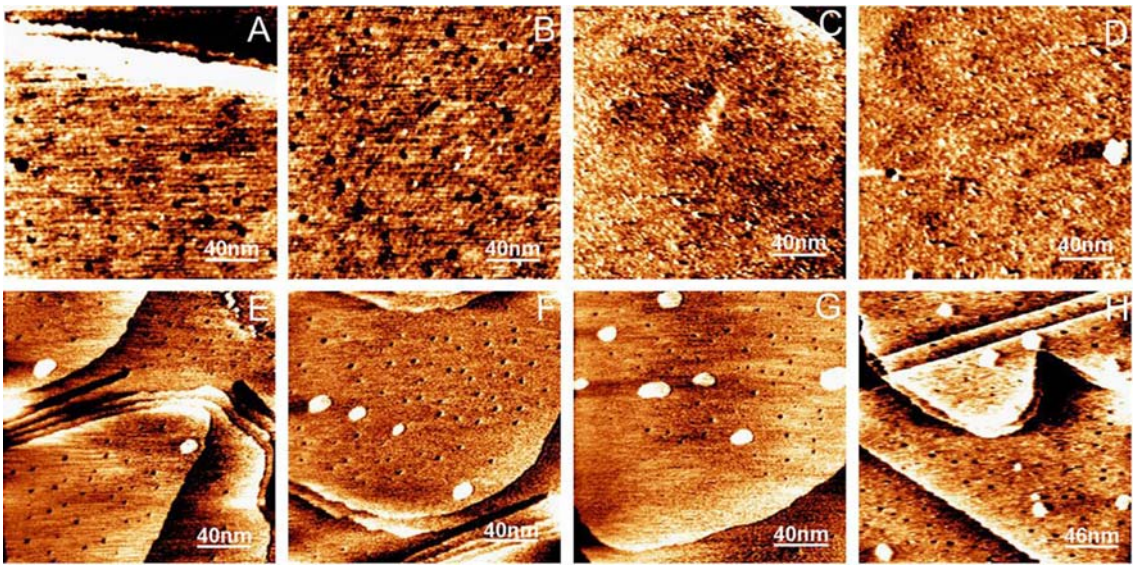

Fig. S1. STM images obtained in 0.1M (A, B, C, D) and 4M (E, F, G, H) $MgCl_2$ solutions. Panel A, B, E, F and C, D, G, H show the images scanned in solutions and in air, respectively. The white spot in panel d exhibits the only aggregation spot observed among a few images in air at 0.1M $MgCl_2$. In 4M $MgCl_2$ solution, more aggregation spots were observed in g and h compared to e and f due to the scanning in air.

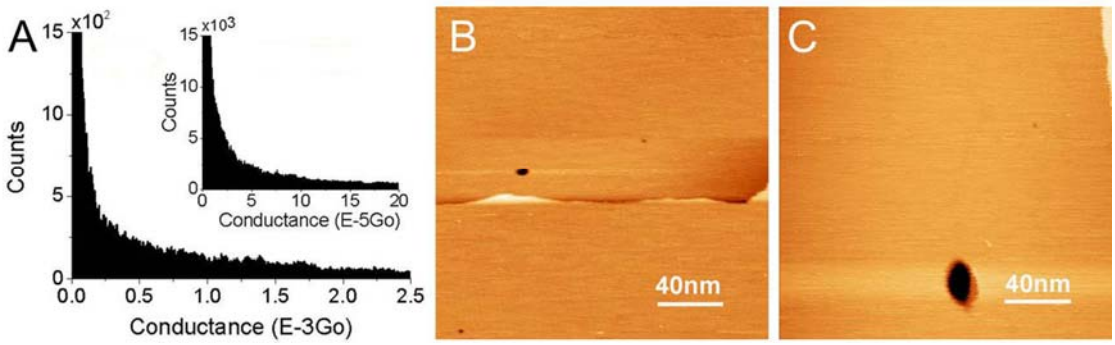

Fig. S2 Conductance measurements and STM imaging in 4M $MgCl_2$ solution containing no DNA molecule. (A) CSM conductance measurements under two linear measurement windows (50mV/div and 1V/div); (B) STM imaging in 4M $MgCl_2$ solution containing no DNA molecule; (C) STM imaging in air for the same sample used in (B) after dried with high purity Nitrogen.

In **Fig. S2a**, under two window scales (1V/div and 50mV/div), histograms constructed from conductance measurements of pure 4M $MgCl_2$ solution containing no DNA molecule showed no prominent peak but a trend of smooth decay, which suggests that the peaks revealed in samples containing DNA molecules were dominantly contributed by DNA molecules rather than other things like salt, water and counterions in the solution.

S5. Estimation on numbers of Mg^{2+} around DNA molecules in 0.1M and 4M $MgCl_2$ sample solution

Previous studies[9, 10] about the crystal structure of Z-DNA suggested that Mg^{2+} could bind to guanine bases, and the phosphate groups through its hydration shell with hydrogen bonds. A certain number of magnesium ions are required to stabilize DNA in Z-conformation. In our case, to briefly estimate the change in the available number of ions per single DNA junction as $MgCl_2$ concentration gradually increases, we approximated a single Au-DNA-Au junction as a cylinder: the outer wall area of the cylinder can be simply defined as the potential binding sites of Mg-water complexes. Taking the volume of the solution (200 μl) and concentration (3 μM) of DNA molecules into account, only the ions within the volume covering the monolayer of DNA molecules impact the conductance measurement. Hence, the whole surface area where DNA monolayer was formed upon Au-S interaction and the length of a single DNA molecule are used as the bottom area and height respectively for the

effective volume calculation. Base on this calculation, at 0.1M $MgCl_2$, there is on average 0.8 Mg^{2+} ion around a single DNA junction, which is apparently not enough to stabilize DNA molecules in Z-conformation as revealed in our conductance measurements. But it is still possible that a few DNA molecules exist in Z-form due to this small amount of $MgCl_2$ injection. On average 8.0 Mg^{2+} ions are available to bind to a single DNA molecule at 1M and even more ions are possible to appear at the surrounding area of a single DNA junction as the concentration increases. It has to be noted that the dynamic movement of Mg^{2+} ions in solution greatly lowers the binding opportunity between ions and DNA. This means that fewer Mg^{2+} ions are indeed able to bind with DNA molecules than the number of ions that appear around the molecule to stabilize it in Z-form. Besides, a couple of magnesium ions could form clusters at specific sites to bind with DNA. Thus, it is plausible that higher concentrations (3M, 4M) of Mg^{2+} are necessary to transfer most DNA molecules and stabilize them in Z-form.

S6. Transition degree (TD) calculation

SHM SPMBJ technique predicts that each plateau in every conductance trace is ideally equal in duration due to the constant 33 ms pause, though the position changes. Therefore, each SHM conductance trace can be regarded as equally contributing to the final SHM conductance histogram. This means that the histogram built from these traces is composed of a finite number of equally sized plateaus, the position of which is concentration dependent. As mentioned in main text, two different measurement regions specifically for two conformations were applied: window 1 for B-DNA and window 2 for Z-DNA, respectively. Since window 1 window washed out plateaus in window 2 and window 2 was too limited to show plateaus in 1 window, one of the two windows failed to show significant information in the other window.

To clarify the transition degree determined upon SHM conductance measurement, **Fig. S3** is shown as an example. By collecting same amount of traces under two measurement regions (50mV/div and 1V/div), the number of Z- and B-DNA junctions formed within the duration of conductance measurement can be specifically interpreted as area (the sum of counts) underneath the first peak in the histograms since plateaus contributed equally to final

histograms. The reason for not considering the second peak is because the second peak is usually not pronounced enough (close to the baseline trend), which suggests a very small signal-noise ratio. Since the second peak indicates two molecules, the inclusion of the area underneath the second peak needs to double the counts, which also doubles the noise and greatly increase the calculation error. Although slight error existed because of the second or third peak differences in the histograms, the main trend of ratio variation between B- and Z-DNA along the rise of $MgCl_2$ concentration kept the same. Here, by summing up the counts in the green line surrounded area under both windows we obtained A_Z and A_B which independently shows the number of Z-DNA junctions and B-DNA junctions, respectively. Since same total number of traces was applied for constructing histograms, the ratio A_Z/A_B briefly represents the proportion of the number of Z-DNA junctions over the number of B-DNA junctions. Thus, $A_Z/(A_B+A_Z)$ indicates the ratio of Z-DNA junction appeared among all DNA junctions in the measurement, which we defined as the transition degree.

Detailed results for each $MgCl_2$ concentration are shown in **Table S1**. TD calculation merely based on conductance measurement only increased up to 80.6%. This is because of the measurement defect. Under either window, systematic signal may generate randomly distributed plateaus which also contributed to final histograms and those near the position of B- or Z-DNA plateaus were undistinguishably counted as real molecular junctions. Therefore, we normalized the transition degree data points and then fitted them by Boltzmann fitting. We chose Boltzmann fitting because it gives not only the transition midpoint, but also the bottom and top asymptotes. Boltzmann fitting suggested that the transition already reached the saturation level at 4M.

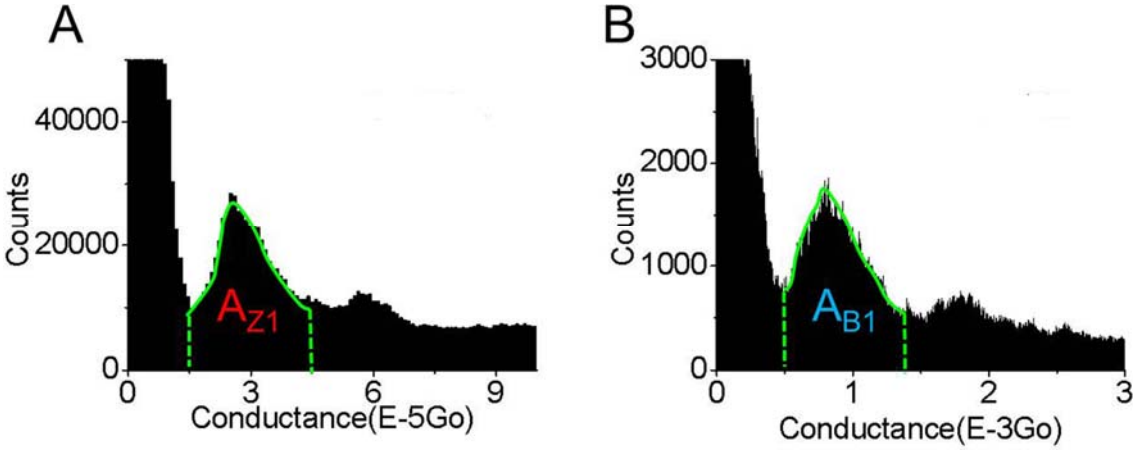

Fig. S3 Panel A and B show conductance histograms constructed from two linear measurement regions: 50mV/div and 1V/div, respectively, in 1M $MgCl_2$ solution. Same amount of conductance traces (~1000) were collected under both windows. Data areas used for TD calculation are circled by dashed and solid lines.

Table S1. Data used for SHM-TD calculation under different $MgCl_2$ concentration

$MgCl_2$ concentration(M)	**A_B (1V/div)**	**A_Z (50mV/div)**	**(A_Z/A_Z+A_B)**	**Normalized Transition Degree**
0.01	-	-	0%	0%
0.1	672517	42927	6.0%	7.5%
0.5	782370	340938	29.9%	37.5%
1.0	769862	617780	44.5%	56.3%
1.5	343838	441804	56.2%	70%
2.0	393870	478876	59.6%	74.5%
3.0	180458	420468	70.4%	90%
4.0	149864	612424	80.3%	100%

Table S2. Transition degree (TD) calculated from SHM conductance measurement and CD measurement

$MgCl_2$ concentration(M)	**0.01**	**0.1**	**0.5**	**1.0**	**1.5**	**2.0**	**3.0**	**4.0**
SHM-TD(%)	0	7.5	37.5	56.3	70.0	74.5	90.0	100.0
CD-TD(%)	0	13.0	36.6	60	65.6	71.0	—	—

From **Table S2**, SHM-TD suggests there is still a rather significant area under the Z-DNA conditional histogram. This inconsistency can be from two reasons: 1) because of the statistical nature of histograms, even a sample of entirely B-DNA will have a small fluctuation which will masquerade as Z-DNA on a conductance trace, 2) DNA is effected by thermal fluctuations and even in a supposed all B-DNA sample, there is going to be some

Z-DNA present, especially in a room temperature buffer.

Table S3. pH values in solutions containing different concentrations of $MgCl_2$

$MgCl_2$ concentration (M)	0	0.1	1.0	2.0	3.0	4.0
pH	7.4	6.9	5.6	4.5	3.2	3.0

References

1. F. M. Pohl and T. M. Jovin, *J. Mol. Biol.*, 1972, 67, 375.
2. J. H. Van De Sande, L. P. McIntosh and T. M. Jovin, *Embo. J.*, 1982, 1, 777-782.
3. Z. Huang, B. Xu, Y. Chen, M. Di Ventra and N. Tao, *Nano Lett.*, 2006, 6, 1240-1244.
4. I. Horcas, R. Fernandez, J. M. Gomez-Rodriguez, J. Colchero, J. Gomez-Herrero and A. M. Baro, *Rev. Sci. Instrum.*, 2007, 78.
5. G. Zheng, X. Lu and W. K. Olson, *Nucleic Acids Res.*, 2009, 37, W240-W246.
6. E. F. Pettersen, T. D. Goddard, C. C. Huang, G. S. Couch, D. M. Greenblatt, E. C. Meng and T. E. Ferrin, *J. Comput. Chem.*, 2004, 25, 1605-1612.
7. D. A. Case, T. A. Darden, T. E. Cheatham III, C. L. Simmerling, J. Wang, R. E. Duke, R. Luo, M. Crowley, R. C. Walker, W. Zhang, K. M. Merz, B. Wang, S. Hayik, A. Roitberg, G. Seabra, I. Kolossvary, K. F. Wong, F. Paesani, J. Vanicek, J. Liu, X. Wu, S. R. Brozell, T. Steinbrecher, H. Gohlke, Q. Cai, X. Ye, J. Wang, M.-J. Hsieh, G. Cui, D. R. Roe, D. H. Mathews, M. G. Seetin, C. Sagui, V. Babin, T. Luchko, S. Gusarov, A. Kovalenko and P. A. Kollman, Unversity of California, San Francisco., 2010.
8. P. Makk, D. Tomaszewski, J. Martinek, Z. Balogh, S. Csonka, M. Wawrzyniak, M. Frei, L. Venkataraman and A. Halbritter, *ACS Nano*, 2012, 6, 3411-3423.
9. R. V. Gessner, C. A. Frederick, G. J. Quigley, A. Rich and A. H. J. Wang, *J. Biol. Chem.*, 1989, 264, 7921-7935.
10. R. V. Gessner, G. J. Quigley, A. H. J. Wang, G. A. Vandermarel, J. H. Vanboom and A. Rich, *Biochemistry*, 1985, 24, 237-240.